Open access • Proceedings Article • DOI:10.1115/DETC2011-47117

Accuracy Evaluation of PRBM for Predicting Kinetostatic Behavior of Flexible Segments in Compliant Mechanisms — Source link

Guimin Chen, Aimei Zhang

Institutions: Xidian University

Published on: 01 Jan 2011

Topics: Compliant mechanism

Proceedings of the ASME 2011 International Design Engineering Technical Conferences & Computers and Information in Engineering Conference
IDETC/CIE 2011
August 28-31, 2011, Washington, DC, USA

DETC2011-47117

ACCURACY EVALUATION OF PRBM FOR PREDICTING KINETOSTATIC BEHAVIOR OF FLEXIBLE SEGMENTS IN COMPLIANT MECHANISMS

Guimin Chen*
School of Mechatronics
Xidian University
Xi'an, Shaanxi, 710071
China
guimin.chen@gmail.com

Aimei Zhang
School of Mechatronics
Xidian University
Xi'an, Shaanxi, 710071
China
amzhang@xidian.edu.cn

ABSTRACT

The pseudo-rigid-body model (PRBM) method has been widely accepted as one of the most important tools for synthesis and analysis of compliant mechanisms. However, the lack of quantitative study on the accuracy of PRBM for predicting the kinetostatic behavior of flexible members always makes users feel unconfident in the results achieved by PRBM. In this paper, a strain-energy-based approach is proposed for evaluating the accuracy of PRBM for predicting kinetostatic behavior of flexible segments, which compares the results of strain energy calculate using PRBM to those obtained using the derived closed-form solutions. The approach was used to evaluate the accuracy of the PRBM for flexible cantilever beams. It is proved that the PRBM is accurate for modeling segments subject to end-moment loads. A thorough comparison for segments subject to end-force loads is also presented. The results could be useful for PRBM users to assess the accuracy of the models for their compliant mechanism designs, or to choose appropriate values for the characteristic parameters. The results may also be used to improve the PRBM.

1 Introduction

Compliant mechanisms, which achieve at least some of their mobility from the deflection of flexible segments rather than from articulated joints only, offer many advantages such as energy storage, increased precision, and reduced wear, backlash and part number. Since many of the flexible segments undergo large deflection, the major challenge of compliant mechanisms lies in the difficulty modeling the nonlinear deflection [1].

The pseudo-rigid-body model (PRBM) method [1], which approximates the nonlinear deflection as motion of rigid links, bridges the gap between compliant mechanisms and rigid-body mechanisms. Due to its straightforwardness and effectiveness, PRBM has been accepted as one of the most important tools for synthesis and analysis of compliant mechanisms. The use of PRBM enables us to apply the knowledge available in the field of rigid-body mechanism to compliant mechanisms. So far, PRBM had been successfully used for identifying multistability [2, 3], characterizing dynamic behaviors [4, 5] and achieving static balancing [6] of compliant mechanisms.

The characteristic parameters of PRBM were determined by first finding the characteristic radius factor (γ) that best fits the tip locus of flexible members (i.e., to maximize the maximum pseudo-rigid-body angle by limiting the relative deflection error of the tip less than 0.5% [1]), and then using it to compute the approximate values for the stiffness coefficient (K_Θ) and the parametric angle coefficient (c_θ). That is to say, the principle objective of PRBM is to accurately predict the kinematic behavior of flexible members (without considering their stiffness behavior). Because there lacks of quantitative study on how accurate could PRBM be in predicting the kinetostatic behavior (namely the force-deflection behavior) of flexible members subject to different load modes or in deflected configurations, users sometimes

*Address all correspondence to this author.

feel unconfident in the results produced by PRBM thus are reluctant to use it, which provides the motivation of this work.

In this work, we propose to use strain energy as the metric for accuracy evaluation of PRBM in predicting the kinetostatic behavior of flexible members due to the following reasons. First, by using the strain energy modeling approach, one can neglect the details of the internal loads and the load equilibrium in flexible members. Second, by taking the first derivative of the strain energy stored in a compliant mechanism, one can achieve the corresponding force-deflection behavior easily. Third, studying strain energy modeling approaches can benefit the research on characterizing dynamic behaviors of compliant mechanisms. Fourth, strain energy modeling based on PRBM (SE-PRBM for short) has already been studied [5] and used in analysis and design of compliant mechanisms. Therefore, the accuracy of PRBM in predicting the kinetostatic behavior may be assessed by comparing the results of SE-PRBM to those obtained using other analysis methods. Among various methods for modeling nonlinear deflections, the elliptic-integral solution is often considered as the most accurate one and had been used as the exact solution in determining the characteristic parameters of PRBM [1]. Based on the Euler-Bernoulli beam theory, we derive the closed-form solution for stain energy of large deflection using the elliptic-integral approach and use it for the accuracy evaluation of SE-PRBM.

It should be noted that the proposed method can also be used to evaluate the accuracy of other PRBM variants, for example, the PRBMs discussed in Refs. [8–13]. A brief summary of the work on various PRBMs can be found in Ref. [14].

The outline of this paper is as follows. Section 2 provides a brief summary of the PRBM for cantilever beams and presents the equations of SE-PRBM. Section 3 derives the elliptic-integral solution for stain energy stored in beams undergo large deflections based on the Euler-Bernoulli beam theory. Section 4 compares the results of SE-PRBM to those of the closed-form solutions and presents the accuracy evaluation of PRBM. The last section has concluding remarks.

2 The pseudo-rigid-body model (PRBM)

The solutions to the large-deflection equations show that the deflected tip locus for a flexible cantilever beam subject to an end force or an end moment is nearly a circular arc (as shown in Figure 1(a)), therefore, PRBM developed by Howell and Midha [1] uses a rigid link rotating around a "characteristic pivot" (i.e., a revolving joint) to approximate the tip locus, as shown in Figure 1(b). A torsional spring is attached to the characteristic pivot to approximate the stiffness of the beam. The PRBM uses three characteristic parameters to identify kinematic and force-deflection characteristics of a flexible segments, namely, the characteristic radius factor (γ), the stiffness coefficient (K_Θ), and the parametric angle coefficient (c_θ). The characteristic pivot is located at a length of γL (the characteristic radius) from the beam tip in its undeflected position, where L is the length of the beam.

The characteristic radius factor γ was found by best fitting the tip locus of flexible members without considering their stiffness behavior. Once γ is determined, the tip position of the deflected beam can be parameterized in terms of the pseudo-rigid-body angle, Θ. The parametric angle coefficient c_θ represents the ratio of θ_o (the beam tip angle) to Θ, namely,

$$\theta_o = c_\theta \Theta \tag{1}$$

There is a nearly linear relationship between θ_o and Θ, thus c_θ can be approximated as a constant for a given loading condition. The stiffness coefficient K_Θ is a nondimensionalized torsional spring constant to model the beam's resistance to deflection. Once K_Θ is determined, the spring stiffness of the equivalent torsion spring, K, can be calculated as

$$K = \gamma K_\Theta \frac{EI}{L} \tag{2}$$

where EI is referred to as the flexural rigidity of the beam.

Table 1. Numerical values for γ, c_θ, K_Θ and $\Theta_{\max}$ for different n (selected from Ref. [1]).

n	γ	c_θ	K_Θ	$\Theta_{\max}$ (K_Θ)
-1	0.8707	1.2323	2.7282	31.5
0	0.8517	1.2385	2.6762	58.5
1	0.8360	1.2467	2.6126	67.5
2	0.8276	1.2511	2.5971	69.0
5	0.8192	1.2557	2.5625	67.5
10	0.8156	1.2578	2.5660	69.7

2.1 Segment subject to an end-force

When an end force (which is decomposed into a verticle component P and a horizontal force nP, as shown in Figure 1(a)) is applied , γ, K_Θ and c_θ can be represented as functions of n (or the force direction angle ϕ). Table 1 lists some numerical values for γ, c_θ and K_Θ for different values of n. Because the values for these characteristic parameters do not vary much over a large range of n, their averaged values, i.e., $\gamma = 0.85$, $K_\Theta = 2.65$

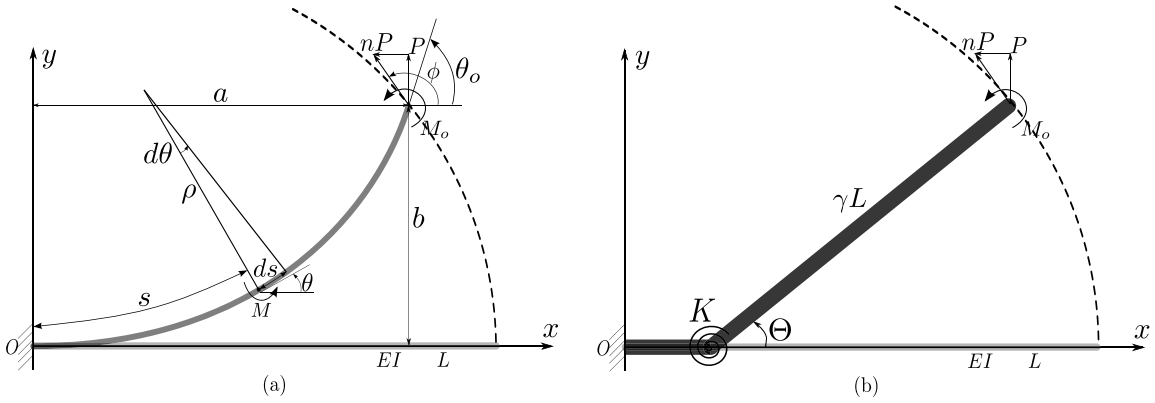

Figure 1. (a) A cantilever beam subject to a combined end force and moment at the free end, and (b) its PRBM.

and $c_\theta = 1.24$, are often used for convenience. The strain energy stored in the beam's PRBM (SE-PRBM) can be approximated as

$$U_P = \frac{1}{2} K \Theta^2 \tag{3}$$

Because the moment at the characteristic pivot is given as

$$M_p = \gamma L(n \sin\Theta + \cos\Theta)P = K\Theta \tag{4}$$

for a known end force (n and P), we can solve Eq. (4) for Θ, then use Eq. (3) to calculate U_P.

Eq. (3) can also be rewritten as

$$U_P = \frac{1}{2}\gamma L(n \sin\Theta + \cos\Theta)P\Theta \tag{5}$$

2.2 Segment subject to an end-moment

For a pure moment load M_o, the characteristic parameters of PRBM are given as: $\gamma = 0.7346$, $K_\Theta = 2.0643$, and $c_\theta = 1.5164$ [1]. The strain energy stored in the beam's PRBM (SE-PRBM) can be calculated as [5]

$$U_M = \frac{1}{2} c_\theta K \Theta^2 \tag{6}$$

Because $M_o = K\Theta$ and $K = \gamma K_\Theta EI/L$, Eq. (6) can be rewritten as

$$U_M = \frac{c_\theta M_o^2}{2\gamma K_\Theta EI/L} \tag{7}$$

3 Closed-form Solutions for Strain Energy

This section derives the closed-form solutions for stain-energy modeling of large-deflection beams. The solution for pure end-moment load is obtained using simple integral techniques, while the solution for pure end-force load is derived based the elliptic-integral approach.

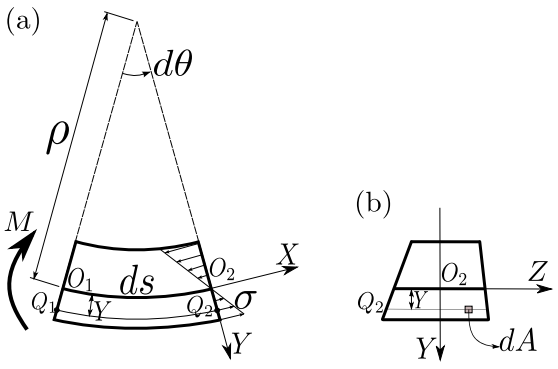

Figure 2. The strain and stress of infinitesimal ds

The Euler-Bernoulli beam theory is based on the assumption that cross-sections remain plane and perpendicular to the longitudinal fibers of the beam during bending. As a result of bending, the top fibers of the beam is extended while the bottom is compressed, as illustrated in Figure 2(a). It is reasonable to suppose that somewhere between the two there is a fiber layer that is neither extended nor compressed (the stress is zero) [15]. This layer is called the neutral layer, and it always pass through the centroid of the cross-section. The radius of curvature R is then measured to the neutral axis.

For infinitesimal ds shown in Fig. 2(a), O_1O_2 is the neutral

layer, ρ is the curvature radius of the neutral layer, $d\theta$ is the angular displacement of the infinitesimal (between the two cross sections). The curvature radius of the top fibers is less than ρ due to compression, while that of the bottom fibers greater than ρ due to elongation. The lengthways fiber with a distance of Y from the neutral layer Q_1Q_2 is elongated by

$$\varepsilon = \frac{(\rho + Y)d\theta - \rho d\theta}{\rho d\theta} = \frac{Y}{\rho} \tag{8}$$

that is to say, the strain of fiber is proportional to the distance (Y) from the neutral axis. According to the law of Hooke, Q_1Q_2:

$$\sigma = E\varepsilon = E\frac{Y}{\rho} \tag{9}$$

For an infinitesimal length ds,

$$\begin{aligned} dV &= \left(\int_A \frac{\sigma^2}{2E} dA\right) \cdot ds = \left(\int_A \frac{(EY/\rho)^2}{2E} dA\right) \cdot ds \\ &= \frac{E}{2\rho^2}\left(\int_A Y^2 dA\right) \cdot ds = \frac{EI}{2\rho^2} \cdot ds \end{aligned} \tag{10}$$

where A is the area of the cross-section, Y is the distance of area infinitesimal dA from the neutral axis, and $I = \int_A Y^2 dA$ is area moment of inertia of the beam cross-section about the neutral axis.

The Euler-Bernoulli beam theory states that the bending moment is proportional to the beam curvature, that is

$$M = EI\frac{d\theta}{ds} = \frac{EI}{\rho} \tag{11}$$

By replacing EI/ρ in Eq. (10) by the bending moment M, we get

$$dV = \frac{M^2}{2EI} \cdot ds \tag{12}$$

Therefore, the total strain energy stored in the beam can be expressed as (note that M is different from M_o)

$$V = \int_0^L dV = \int_0^L \frac{M^2}{2EI} ds \tag{13}$$

3.1 Elliptic-integral solution for segment subject to an end-force

Eq. (13) can be rewritten as

$$V_P = \int_0^L \frac{M^2}{2EI} ds = \int_0^L \frac{1}{2EI}\left(EI\frac{d\theta}{ds}\right)^2 ds = \int_0^L \frac{EI}{2}\left(\frac{d\theta}{ds}\right)^2 ds \tag{14}$$

According to the derivation in Ref. [1], the curvature of a beam subject an end-force load can be expressed as

$$\frac{1}{\rho} = \frac{d\theta}{ds} = \sqrt{\frac{2P}{EI}(\lambda - \sin\theta + n\cos\theta)} \tag{15}$$

where

$$\lambda = \sin\theta_o - n\cos\theta_o \tag{16}$$

Eq. (15) can also be rewritten as

$$ds = \frac{d\theta}{\sqrt{\frac{2P}{EI}(\lambda - \sin\theta + n\cos\theta)}} \tag{17}$$

Substituting Eqs. (15) and (17) into Eq. (14) yields

$$V_P = \sqrt{\frac{PEI}{2}} \int_0^{\theta_o} \sqrt{\lambda - \sin\theta + n\cos\theta} d\theta \tag{18}$$

We denote that

$$N = \int_0^{\theta_o} \sqrt{\lambda - \sin\theta + n\cos\theta} d\theta \tag{19}$$

which will be solved using the elliptic-integral approach in the following.

We define the following transformation

$$\mathrm{sn}^2(u,t) = \frac{\eta + \sin\theta - n\cos\theta}{\lambda + \eta} \tag{20}$$

where sn is one of the Jacobian elliptic functions, t the elliptic modulus given as

$$t = \sqrt{\frac{\lambda + \eta}{2\eta}}$$

and

$$\eta = \sqrt{1 + n^2}$$

Differentiating Eq. (20) with respect to θ and simplifying yields

$$d\theta = \sqrt{\frac{2}{\eta}} \sqrt{\lambda - \sin\theta + n\cos\theta} du \tag{21}$$

Substituting Eq. (21) into Eq. (19) results in

$$\begin{aligned} N &= \sqrt{\frac{2}{\eta}} \int_{u_1}^{u_2} (\lambda - \sin\theta + n\cos\theta) du \\ &= \sqrt{\frac{2}{\eta}} \{2\eta[E(t) - E(\gamma,t)] + (\lambda - \eta)[F(t) - F(\gamma,t)]\} \end{aligned} \tag{22}$$

where

$$\gamma = \sin^{-1}\sqrt{\frac{\eta - n}{\lambda + \eta}}$$

$$\mathrm{sn}(u_1, t) = \sin\gamma$$

and

$$\mathrm{sn}(u_2, t) = 1$$

$F(\gamma,t)$ and $E(\gamma,t)$ are the elliptic integrals of the first and second kind, and $F(t)$ and $E(t)$ are the complete elliptic integrals of the first and second kind.

Substituting Eq. (22) into Eq. (18) yields

$$V_P = \sqrt{\frac{PEI}{\eta}} \{2\eta[E(t) - E(\gamma,t)] + (\lambda - \eta)[F(t) - F(\gamma,t)]\} \tag{23}$$

Because (see Ref. [1], Eqs. (2.83) and (2.90))

$$\begin{aligned} \sqrt{\frac{PL^2}{EI}} &= \frac{1}{\sqrt{2}} \int_0^{\theta_o} \frac{d\theta}{\sqrt{\lambda - \sin\theta + n\cos\theta}} \\ &= \frac{1}{\sqrt{\eta}} [F(t) - F(\gamma,t)] \end{aligned} \tag{24}$$

by substituting Eq. (24) into Eq. (23) and eliminating P, V_P can be rewritten as

$$\begin{aligned} V_P &= \frac{EI}{L} \{2[E(t) - E(\gamma,t)][F(t) - F(\gamma,t)] + \frac{\lambda - \eta}{\eta} [F(t) - F(\gamma,t)]^2\} \\ &= \frac{EI}{L} \cdot f(n, \theta_o) \end{aligned} \tag{25}$$

3.2 Solution for segment subject to an end-moment

For pure moment load (M_o at the free end), the bending moment is constant along the beam and the deflected beam exhibits a circular arc with a constant curvature. The strain energy stored in the beam can be calculated as

$$V_M = \int_0^L \frac{M_o^2}{2EI} ds = \frac{M_o^2 L}{2EI} \tag{26}$$

4 Accuracy Evaluation

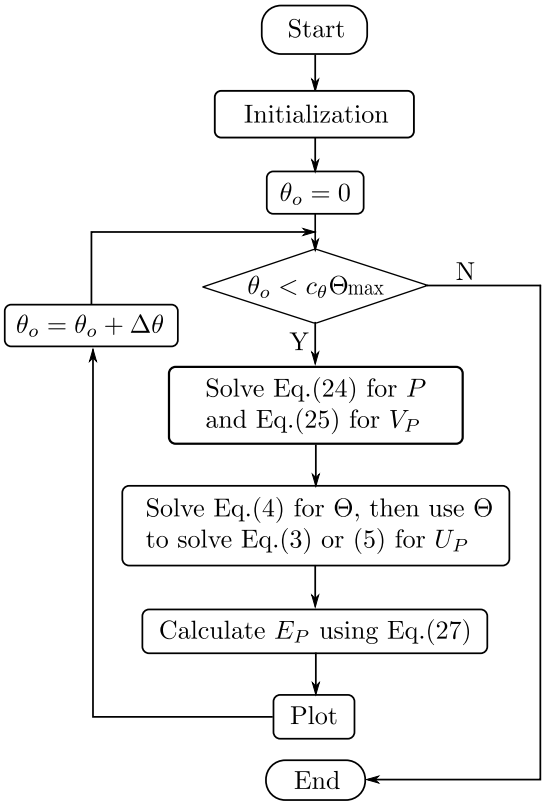

Figure 3. Flowchart for the comparison calculation.

In this section, the accuracy of PRBM for predicting kinetostatic behaviors is evaluated by comparing the results of SE-PRBM to those of the closed-form solutions derived in Section 3. The nondimensionalized error of PRBM for modeling the strain energy of cantilever beams is defined as (compared to the elliptic-integral solution)

$$E_P = \frac{U_P - V_P}{V_P} \times 100\% \tag{27}$$

In the comparison, the following values for the beam's properties are used: $L = 0.03$ m and $EI = 1.067 \times 10^{-4}$ N·m^2. The force P was increased step by step until Θ reaches $\Theta_{\max}$ given in Table 1.

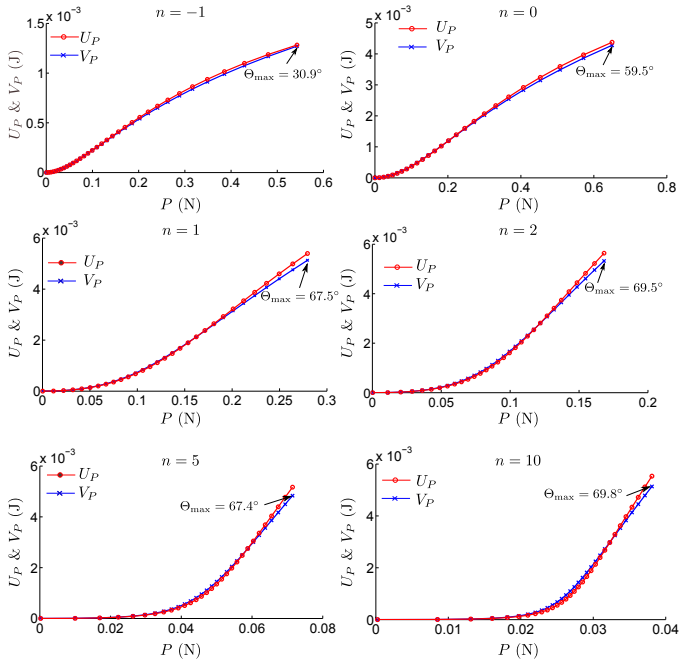

Figure 4. Strain energy versus P for different n (U_P was calculated using the numerical values for the characteristic parameters given in Table 1).

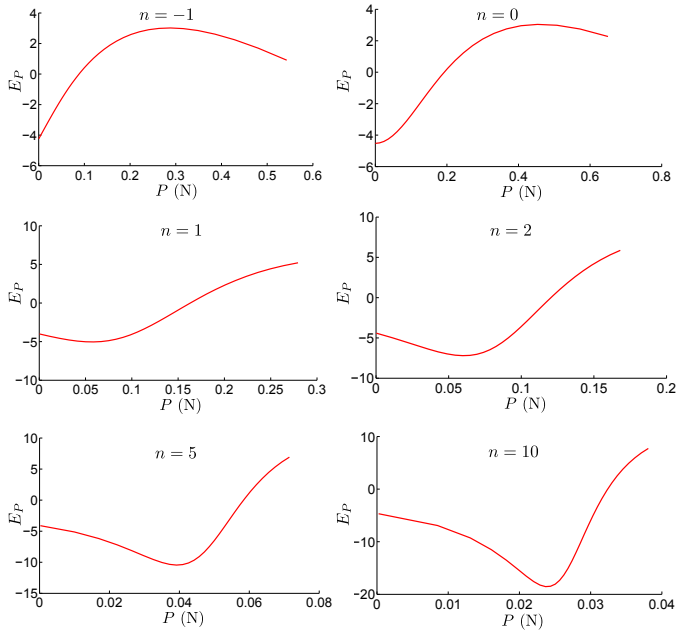

Figure 5. Plot of E_P versus P for different n (U_P was calculated using the numerical values for the characteristic parameters given in Table 1).

4.1 Comparison for end-force load (under equal load)

This subsection conducts the comparison by applying equal end-force to both the cantilever beam and its PRBM. The flowchart for the comparison calculation is shown in Figure 3.

We first compare the SE-PRBM employing the numerical values listed in Table 1 as its characteristic parameters to the elliptic-integral solution under the same load condition. The curves for U_P and V_P versus P are plotted in Figures 4 for different n. Figure 5 shows the corresponding E_P.

Second, we compare the SE-PRBM employing the averaged values as its characteristic parameters (i.e., $\gamma = 0.85$, $K_\Theta = 2.65$ and $c_\theta = 1.24$) to the elliptic-integral solution with equal end-force load. Figures 6 plots the curves for U_P and V_P versus P for different n, and the corresponding E_P is shown in Figure 7.

From the results shown in Figures 4-7, we may conclude that:

1. In general, the PRBM using different values for its characteristic parameters is more accurate in predicting kinetostatic behavior than the PRBM with the averaged values.
2. In most cases, the error of PRBM stays within 10 percent of the results obtained by the elliptic integral solution in predicting the kinetostatic behavior of flexible segments.
3. When the horizontal component (nP) dominates the end force (e.g., $n = 10$), the error may be rather large (the maximum error is nearly 18 percent for the PRBM using different values for its characteristic parameters, and 30 percent for the PRBM with the averaged values).

4.2 Comparison for end-force load (under equal tip deflections, i.e., a and b)

The comparison presented in this subsection is conducted by setting both the cantilever beam and its PRBM undergo equal tip deflections (allowing for 0.5 percent error of the tip deflections between the beam and its PRBM, as defined in Ref. [1]). Given a set of (a,b) for the beam, the corresponding PRBM angle Θ is determined as [1]

$$\Theta = \arctan \frac{b}{a - L(1-\gamma)} \tag{28}$$

Then Θ is used to calculate the strain energy of the PRBM for comparison. The flowchart for the comparison calculation is shown in Figure 8.

We first compare the SE-PRBM employing the numerical values listed in Table 1 as its characteristic parameters to the

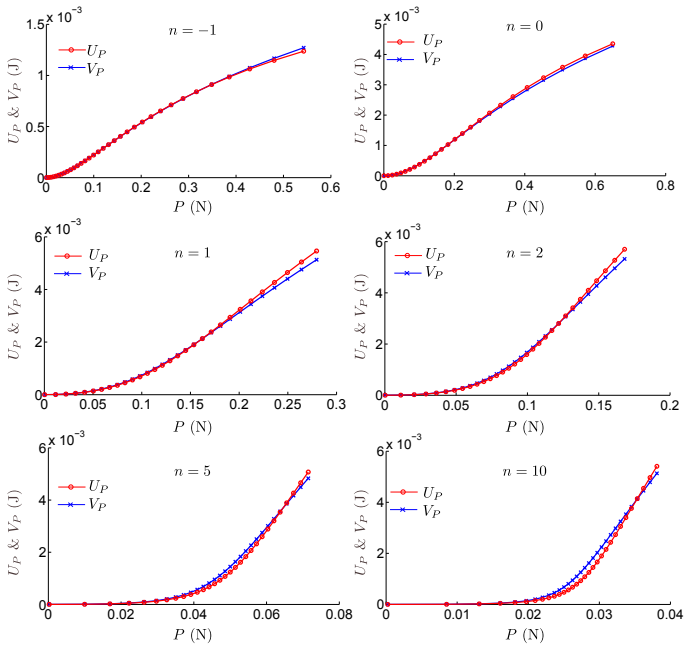

Figure 6. Strain energy versus P for different n (U_P was calculated using the averaged values for the characteristic parameters).

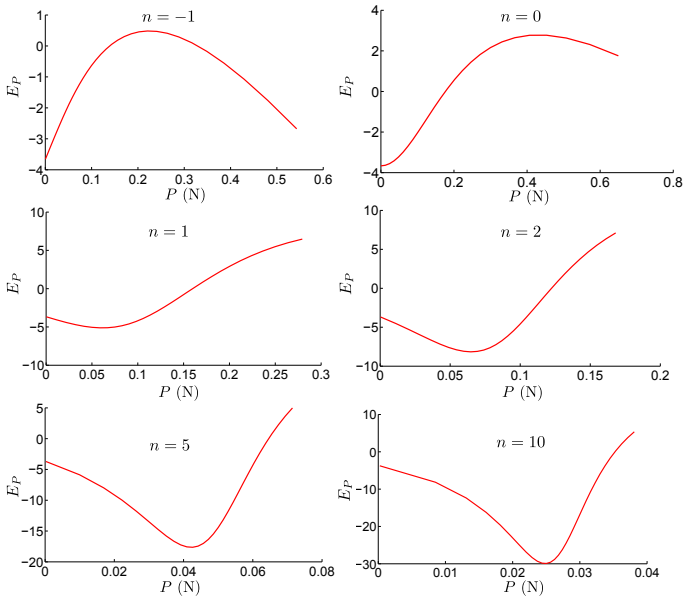

Figure 7. Plot of E_P versus P for different n (U_P was calculated using the averaged values for the characteristic parameters).

elliptic-integral solution. The curves for U_P and V_P versus δ_e are plotted in Figures 9 for different n, where δ_e is defined as [1]

$$\delta_e = \sqrt{(L-a)^2 + b^2} \tag{29}$$

Figure 10 shows the corresponding E_P.

Second, we compare the SE-PRBM employing the averaged values as its characteristic parameters (i.e., $\gamma = 0.85$, $K_\Theta = 2.65$ and $c_\theta = 1.24$) to the elliptic-integral solution. Figures 11 plots the curves for U_P and V_P versus δ_e for different n, and the corresponding E_P is shown in Figure 12.

From the results shown in Figures 9-12, we may conclude that:

1. Using the averaged values for its characteristic parameters doesn't deteriorate the approximation accuracy of the PRBM as compared to the PRBM with varying values for different n.
2. The error of predicting the kinetostatic behavior of flexible segments is less than 5 percent.
3. Interestingly, the error decreases as the deflections increase.

4.3 Comparison for end-moment load

By comparing Eq. (7) to Eq. (26), we have

$$U_M = \frac{c_\theta M_o^2}{2\gamma K_\Theta EI/L} = \frac{c_\theta}{\gamma K_\Theta}\frac{M_o^2 L}{2EI} \approx \frac{M_o^2 L}{2EI} = V_M \tag{30}$$

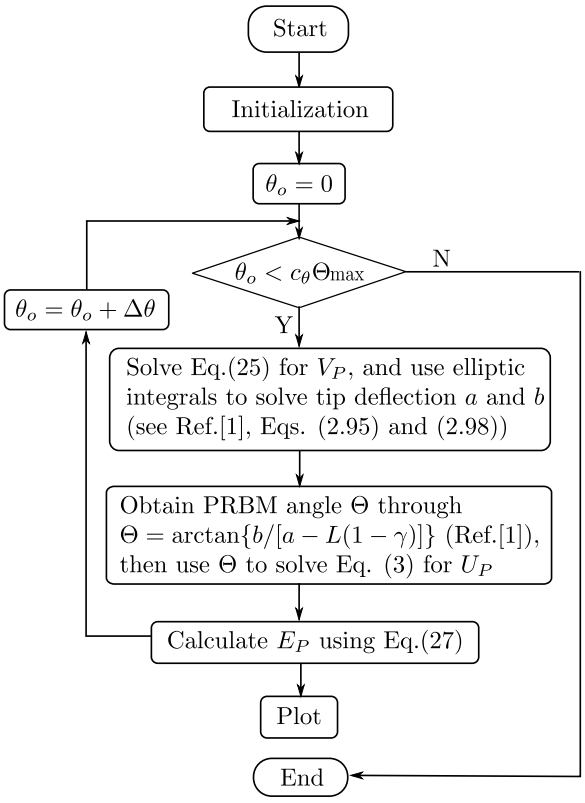

Figure 8. Flowchart for the comparison calculation.

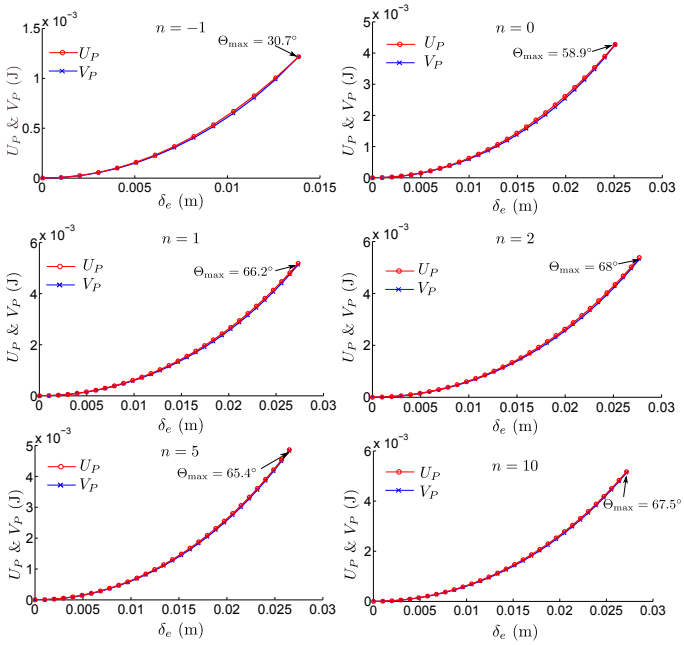

Figure 9. Strain energy versus δ_e for different n (U_P was calculated using the numerical values for the characteristic parameters given in Table 1).

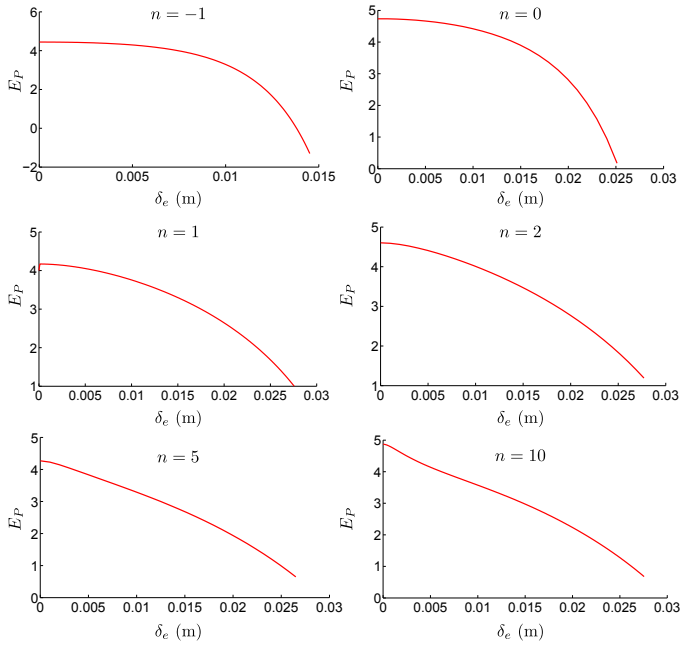

Figure 10. Plot of E_P versus δ_e for different n (U_P was calculated using the numerical values for the characteristic parameters given in Table 1).

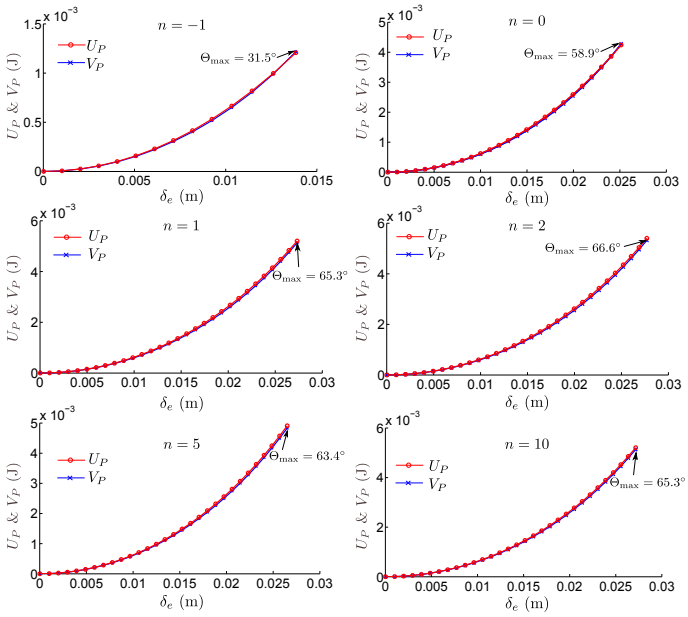

Figure 11. Strain energy versus δ_e for different n (U_P was calculated using the averaged values for the characteristic parameters).

That is to say, PRBM represents an accurate method in predicting the kinetostatic behavior of flexible segments subject to end-moment loads ($\Theta_{\max} = 82.04°$ [1]).

5 Conclusions

We proposed a strain-energy-based approach for evaluating the accuracy of PRBM for predicting kinetostatic behavior of flexible segments. The approach was used to evaluate the accuracy of the PRBM for flexible cantilever beams. It has been proved that the PRBM is accurate for modeling segments subject to end-moment loads. A thorough comparison for segments subject to end-force loads is also presented. The results may be useful for PRBM users to roughly assess the accuracy of the models for their compliant mechanism designs, or to choose appropriate values for the characteristic parameters. It is also possible to use the approach for improving the PRBM.

ACKNOWLEDGMENT

The authors gratefully acknowledge the financial support from the National Natural Science Foundation of China under Grant No. 50805110, the Key Project of Chinese Ministry of Education under No. 109145, and the Fundamental Research Funds for the Central Universities under No. JY10000904010.

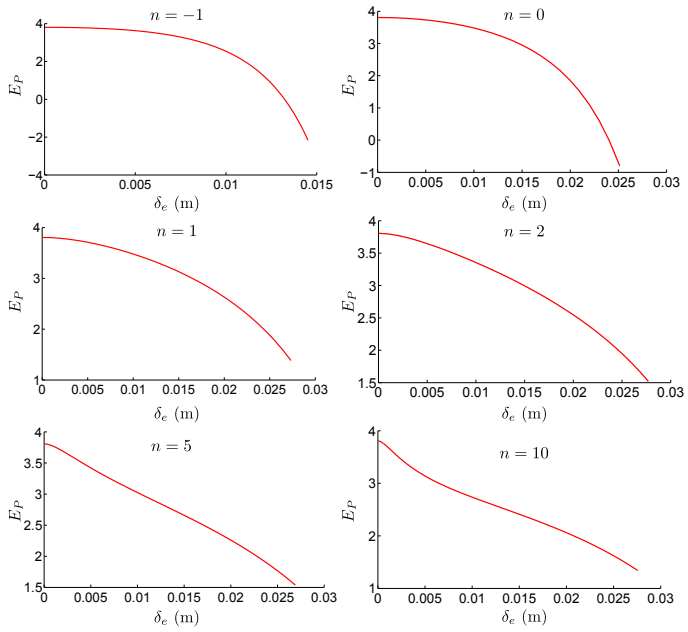

Figure 12. Plot of E_P versus δ_e for different n (U_P was calculated using the averaged values for the characteristic parameters).

REFERENCES

[1] Howell, L. L., 2001, "Compliant Mechanisms," Wiley-Interscience, New York, NY.

[2] Jensen, B. D., and Howell, L. L., 2003, "Identification of compliant pseudo-rigid-body mechanism configurations resulting in bistable behavior," ASME J. Mechan. Des., **125**(4), pp. 701-708.

[3] Chen, G., Wilcox, D. L., and Howell, L. L., 2009, "Fully compliant double tensural tristable micromechanisms (FTTM)," J. Micromech. Microeng, **12**(2), 025011.

[4] Lyon, S. M., Erickson, P. A., Evans, M. S., and Howell, L. L., 1999, "Prediction of the first modal frequency of compliant mechanisms using the pseudo-rigid-body model," ASME J. Mechan. Des., **121**(2), pp. 309-313.

[5] Yu, Y.-Q., Howell, L. L., Lusk, C., Yue, Y., and He, M.-G., 2005, "Dynamic modeling of compliant mechanisms based on the pseudo-rigid-body model," ASME J. Mechan. Des., **127**(7), pp. 760-765.

[6] Gallego, J. A., and Herder, J. L., 2010, "Criteria for the static balancing of compliant mechanisms,"Proceedings of the ASME Design Engineering Technical Conferences & Computers and Information in Engineering Conference, Montreal, Canada, Aug. 15-18, DETC2010-28469.

[7] Midha, A., Howell, L. L., and Norton, T. W., 2000, "Limit positions of compliant mechanisms using the pseudo-rigid-body model concept," Mech. Mach. Theory, **35**(1), pp. 99-115.

[8] Saxena, A., and Kramer, S. N., 1998, "A simple and accurate method for determining large deflections in compliant mechanisms subjected to end forces and moments," ASME J. Mechan. Des., **120**(3), pp. 392-400.

[9] Lyon, S. M., Howell, L. L., and Roach, G. M., 2000, "Modeling flexible segments with force and moment end loads via the pseudo-rigid-body model,"Proceedings of the ASME Internationcal Mechanical Engineering Congress and Exposition, Orlando, FL, Nov. 5-10, DSC-Vol. 69-72, pp. 883-990.

[10] Dado, M. H., 2001, "Variable parametric pseudo-rigid-body model for large-deflection beams with end load," Int. J. Nonlin. Mech., **36**(7), pp. 1123-1133.

[11] Kimball, C., and Tsai, L. W., 2002, "Modeling of flexural beams subjected to arbitrary end loads," ASME J. Mechan. Des., **124**, pp. 223-235.

[12] Lyon, S. M., and Howell, L. L., 2002, "A simplified pseudo-rigid-body model for fixed-fixed flexible segments,"Proceedings of the ASME Design Engineering Technical Conferences, Montreal, Canada, Sept. 29-Oct. 3, DETC2002/MECH-34203.

[13] Su, H.-J., 2009, "A pseudorigid-body 3R model for determining large deflection of cantilever beams subject to tip loads," ASME J. Mech. Robot., **1**(2), 021008.

[14] Chen, G., Xiong, B., and Huang, X., 2011, "Finding the optimal characteristic parameters for 3R pseudo-rigid-body model using an improved particle swarm optimizer," Precis. Eng., **35**(3).

[15] Hearn, E. J., 1977, "Mechanics of Materials," Oxford: Pergamon Press.